




ORIGINAL ARTICLE

Diabetes mellitus type 2 drives metabolic reprogramming to promote pancreatic cancer growth

Guermarie Velazquez-Torres^{1,†}, Enrique Fuentes-Mattei^{1,†}, Hyun Ho Choi^{2,3,†}, Sai-Ching J. Yeung⁴, Xiangqi Meng^{2,*} and Mong-Hong Lee ^{3,*}

¹Department of Molecular and Cellular Oncology, Division of Basic Science Research, The University of Texas MD Anderson Cancer Center, Houston, TX, USA; ²Guangdong Provincial Key laboratory of Colorectal and Pelvic Floor Disease, Sun Yat-sen University, Guangzhou, P. R. China; ³Guangdong Research Institute of Gastroenterology, The Sixth Affiliated Hospital of Sun Yat-sen University, Guangzhou, P. R. China;

⁴Department of Emergency Medicine Division of Internal Medicine, The University of Texas MD Anderson Cancer Center, Houston, TX, USA

*Corresponding authors. Mong-Hong Lee, Guangdong Research Institute of Gastroenterology, The Sixth Affiliated Hospital of Sun Yat-sen University, Guangzhou, Guangdong 510655, China. Tel: +86-20-38455542; Email: vlimh33@mail.sysu.edu.cn; Xiangqi Meng, Guangdong Provincial Key laboratory of Colorectal and Pelvic Floor Disease, Sun Yat-sen University, Guangzhou, Guangdong 510000, China. Tel: +86-20-38455546; Email: mengxq3@mail.sysu.edu.cn

[†]These authors contributed equally to this work.

Abstract

Background: Diabetes mellitus type 2 (DM2) is a modifiable risk factor associated with pancreatic carcinogenesis and tumor progression on the basis of epidemiology studies, but the biological mechanisms are not completely understood. The purpose of this study is to demonstrate direct evidence for the mechanisms mediating these epidemiologic phenomena. Our hypothesis is that DM2 accelerates pancreatic cancer growth and that metformin treatment has a beneficial impact.

Methods: To determine the effect of glucose and insulin in pancreatic cancer proliferation, we used conditioned media to mimic DM2 conditions. Also, we studied the effect of anti-diabetic drugs, particularly metformin and rosiglitazone on pancreatic cancer growth. We established orthotopic/syngeneic (*Lep^r^{ab/db}*) mouse cancer models to evaluate the effect of diabetes on pancreatic tumor growth and aggressiveness.

Results: Our results showed that diabetes promotes pancreatic tumor growth. Furthermore, enhanced tumor growth and aggressiveness (e.g. epithelial-mesenchymal transition) can be explained by functional transcriptomic and metabolomic changes in the mice with diabetes, namely via activation of the AKT/mTOR pathway. Metformin treatment suppressed the diabetes-induced AKT/mTOR pathway activation and tumor growth. The metabolic profile determined by mass spectrum showed important changes of metabolites in the pancreatic cancer derived from diabetic mice treated with metformin.

Conclusions: Diabetes mellitus type 2 has critical effects that promote pancreatic cancer progression via transcriptomic and metabolomic changes. Our animal models provide strong evidence for the causal relationship between diabetes and accelerated pancreatic cancers. This study sheds a new insight into the effects of metformin and its potential as part of therapeutic interventions for pancreatic cancer in diabetic patients.

Key words: pancreatic cancer; type 2 diabetes mellitus; cancer metabolism

Submitted: 1 November 2019; Revised: 17 January 2020; Accepted: 1 March 2020

© The Author(s) 2020. Published by Oxford University Press and Sixth Affiliated Hospital of Sun Yat-sen University

This is an Open Access article distributed under the terms of the Creative Commons Attribution Non-Commercial License (<http://creativecommons.org/licenses/by-nc/4.0/>), which permits non-commercial re-use, distribution, and reproduction in any medium, provided the original work is properly cited. For commercial re-use, please contact journals.permissions@oup.com

Introduction

Pancreatic ductal adenocarcinoma (PDAC) is among the top 10 causes of cancer death worldwide. Pancreatic cancer is projected to be the second leading causes of cancer death by 2030 [1]. Pathological study is a major focus of pancreatic cancer. Recent studies show that even microbiome [2, 3] and fungi [4] have a role in pancreatic cancer development. In addition, many epidemiological studies suggest the important role of diabetes mellitus type 2 (DM2) in carcinogenesis, cancer survival, and as a significant risk factor for PDAC [5]. It is known that gut-microbiota dysbiosis causes diabetes [6], thereby leading to a possibility of influencing the growth of pancreatic cancer. On the other hand, PDAC is also a presumed cause of diabetes due to uncharacterized mechanisms [7]. Thus, these relationships between diabetes and PDAC are very complex, and the mechanisms of pancreatic cancer development under DM2 conditions remain to be further characterized.

Approximately 80% of pancreatic cancer patients have DM2 [8]. Several causes may be involved in the association of DM2 with pancreatic cancer. For example, DM2 demonstrates elevations in circulating insulin and glucose, as well as systemic low-grade inflammations, thereby contributing to cancer initiation/progression [9]. However, the biological mechanisms by which DM2 promotes pancreatic cancer are not completely understood and more studies are needed to confirm diabetes as a risk factor for pancreatic cancer [5, 10]. If DM2 is a risk factor, could anti-insulin-resistance drugs improve the overall survival of pancreatic cancer patients in the context of DM2? If so, what are the mechanisms by which anti-diabetic drugs inhibit pancreatic cancer carcinogenesis at the cellular level? Also, it is possible that specific types of anti-diabetic drug treatments for DM2 may have different impacts on pancreatic cancer based on their mechanisms of action. Alarmingly, the strategy for clinical interventions to improve the outcome of diabetic pancreatic patients has not been established.

In this study, we used the diabetes mouse model *Lep^{db/db}*. The leptin-receptor gene in this mouse model contains a point mutation that results in a stop codon that shortens the intracellular domain and abolishes its signaling capacity [11]. In order to express the disease, it is necessary to have homozygous *Lep^{db/db}*, which is a common mouse model of DM2. Different anti-diabetic drugs, such as insulin/insulin analogs, sulfonylureas, meglitinides, alpha glucosidase inhibitors, thiazolidinediones, biguanides, incretin mimetics, DDP-4 inhibitors, and amylin analogs, are used for diabetes treatment and these drugs have diverse mechanisms of action and targets. Therefore, optimal treatment of DM2 may play a major role in the primary suppression of pancreatic cancer in the presence of diabetes. Metformin improves glycemic control by decreasing the intestinal absorption of glucose and improving insulin sensitivity in muscle and liver tissue [12]. Biguanide drug metformin seems to be ideal for studying its antineoplastic activity [13]. In this study, we focused on the study of metformin, but also used other drugs such as rosiglitazone and exenatide, which have multiple effects on cells independently of glucose metabolism [14, 15]. We established orthotopic/syngeneic (*Lep^{db/db}*) pancreatic cancer mouse models and demonstrate that indeed DM2 accelerates cancer growth and that metformin is effective in suppressing cancer growth. Further, transcriptomic and metabolomics analyses of the tumors from these models demonstrate that the DM2 condition drives metabolic reprogramming to accelerate cancer growth and that metformin

treatment reverts the metabolic reprogramming profile to suppress cancer growth.

In summary, we demonstrate direct evidence for the mechanisms mediating DM2's impact in promoting pancreatic cancer growth. This research work also shed a new insight into the effects of metformin and its potential as part of therapeutic interventions for pancreatic cancer in DM2 patients.

Material and methods

Chemical and reagents

Metformin (Enzo Life Sciences; Farmingdale, NY, USA) was prepared at 400 mM in distilled, deionized autoclaved water and filtered for sterile conditions. Dilutions were prepared in water or media, depending on the experiment. Rosiglitazone (Cayman Chemicals; Ann Arbor, MI, USA) stock was prepared in dimethyl sulfoxide (DMSO) (Fisher; Pittsburg, PA, USA) at a concentration of 100 mM for each experiment. D-Glucose, insulin, and methylthiazolydiphenyl-tetrazolium bromide (MTT) were obtained from Sigma (St. Louis, MO, USA).

Cell culture

MIA PaCa-2, human pancreatic ductal adenocarcinoma cell line, was obtained from the American Type Culture Collection (Manassas, VA, USA). PancO2, pancreatic ductal adenocarcinoma mouse cell line, was kindly provided by Dr Paul Chiao [MD Anderson Cancer Center (MDACC)]. This cell line was established from C57BL/6 mice in 1984 [16]. Cells were maintained in Dulbecco's modified Eagle medium/nutrient mixture F-12 (DMEM/F12; Sigma) supplemented with 10% fetal bovine serum (FBS) (Gemini; West Sacramento, CA, USA) and 1% antibiotic/antimycotic solution [10,000 IU Penicillin (per mL), 10,000 µg/mL streptomycin, 25 µg/mL amphotericin] (Corning Life Sciences Mediatech Inc; Manassas, VA, USA). Cells were kept at 37°C under humid conditions with 5% CO₂.

Media to mimic DM2 conditions

In order to reproduce the glucose and insulin conditions found in diabetes patients, MIA PaCa-2 cells were cultured in different media to perform MTT assays. Normal-condition media was prepared by adding normal serum levels of glucose (100 mg/dL) and insulin (1.23×10^{-3} µM). Diabetes media contained high glucose and high insulin (400 mg/dL and 12.3 µM, respectively) as previously described [15].

Wound-healing assay

MIA PaCa-2 cells were plated and incubated to form a monolayer. Then, a wound (scratch) was performed and indicated treatments were added. Wound closure was monitored by using time-lapse microscopy and images of MIA PaCa-2 cells showed the wound area at different time points of 0, 12, 24, and 36 h. For the quantitation, wound areas at different time points were plotted. Each treatment was normalized with its time 0 h (initial wound area).

Glucose uptake

The fluorescent glucose analog 2-(N-(7-nitrobenz-2-oxa-1,3-diazol-4-yl)amino)-2-deoxyglucose (2-NBDG) was used to determine its uptake into the cells as previously described [17]. Glucose free medium (Life Science Technologies; Grand Island,

NY, USA) containing 120 μ M 2-NBDG and 10% FBS was used to replace the media on the day of the experiments. Images were taken using a fluorescent inverted microscope (Nikon; Melville, NY, USA) before media replacement, 15 min, 30 min, 1 h, and 2 h after 2-NBDG media was added. Fluorescent-microscopy images were taken using a 488-wavelength filter. At the same time points, flow-cytometry analysis to determine the percent of positive fluorescent cells was performed, using a BD FACS Canto II (BD Biosciences; San Jose, CA, USA).

Time-lapse microscopy

For each experiment, cells were treated as described. Cells were plated to form a monolayer and kept in the incubator overnight. Cell wounds were performed inside the biosafety cabinet by using a sterile tip. Then, culture media was replaced for the treatment media containing metformin (5 mM) or rosiglitazone (100 μ M). The microscope (Zeiss; Oberkochen, Germany) was set to keep a temperature of 37°C and 5% CO₂ in a humid environment. Axio Vision Rel 4.6 software was used to set the parameters for the image captured. Several images were taken from each treatment. For each well, three different areas were captured every 30 min over a 36-h time period. A minimum of three biological replicas for each condition were performed. Wound gap was analysed using Image J (software from National Institute of Health; Bethesda, MA, USA).

Extracellular acidification rate (ECAR) and oxygen-consumption rate (OCR) levels using Seahorse

Pancreatic cancer cells were cultured with their respective treatments. For treatments, cells were plated in the XF24 microplate (Seahorse; North Billerica, MA, USA) and treated 24 h before assay. Cells were trypsinized and plated in the XF24 microplate (Seahorse) 8 h before the assay to have a monolayer (20,000 cells per well). Low sodium bicarbonate assay medium pH 7.4 (Seahorse) was prepared the night before running the assay by adding 1 mM sodium pyruvate, 1 mM glutamine, and 25 mM D-glucose placed at 37°C. Cartridge was rehydrated with assay buffer overnight and incubated in a hypoxic incubator. Culture media was replaced for the above-mentioned low sodium bicarbonate assay medium pH 7.4 and equilibrated for 1 h in a hypoxic incubator at 37°C. A series of mitochondrial inhibitors were used to determine the glycolysis and mitochondrial respiration capacities of the cells after the treatments. In order to inhibit the adenosine triphosphate synthase, 10 mM oligomycin (Sigma) was added to determine the mitochondrial-independent oxygen consumption. To determine the maximal respiration, 10 mM hydrophobic acid carbonylcyanide-4-(trifluoromethoxy) phenylhydrazone (FCCP; Sigma), a proton ionophore, was used. Finally, a combination of 10 mM rotenone (Sigma) and antimycin A (Sigma), mitochondrial electron transport inhibitors at complex I and III, respectively, were used to determine the spare respiratory capacity. Inhibitors were sequentially added to establish the ECAR and OCR. Results were analysed using Seahorse XF software (Seahorse). To normalize the results, the protein concentration was determined.

Nude-mice xenograft

Nude mice were maintained in a barrier facility in compliance with all animal care and use guidelines. All animal experiments were performed in accordance with the MD Anderson Institutional Animal Care and Use Committee (IACUC) and approved by the American Association for Laboratory Animal

Science. MIA PaCa-2 cells were injected in the flank of mice at a concentration of 500,000 cells in 200 μ L of PBS. Metformin (1 g/kg/day) and rosiglitazone (1.5 mg/kg/day) were provided in drinking water. Tumor growths were monitored by measuring with a caliper and the tumor volume was estimated by: Length \times Width²/2. Mice were sacrificed before the tumors reach the 1.5-cm mean diameter. Tumors were collected and weighed. Tumors were collected for protein extraction and immunohistochemistry (IHC) analysis as previously described [18, 19].

Diabetic-mouse models

Leptin-receptor heterozygous mutant mouse model *+/Lepr^{db}* mice strain: B6.Cg-*m +/+ Lepr^{db}/J*; stock: 000697, was obtained from Jackson Laboratories (Bar Harbor, MN, USA). C57 BL/6J stock: 000664 wild-type mice were used as breeders. Breeding pairs were obtained from Jackson Laboratories and mice were bred in the institution animal facility following the regulations. Heterozygous leptin-receptor mutant mice *+/Lepr^{db}* were crossed with itself to obtain *Lepr^{db/db}* mice that are diabetic/obese mouse models. To identify the leptin-receptor mutant mice, mouse genotyping was performed. Wild-type littermates were used as experimental controls. These mice were used for the orthotopic syngeneic mouse experiments. All animal experiments were performed in accordance with the IACUC.

Mouse genotyping

Leptin receptor db mutant mice were identified by genotyping. Briefly, mice tails were clipped (0.5 cm) 15 days after birth. Tail snips were incubated with DNA-extraction buffer [100 mM Tris (pH 8.0), 0.2% sodium dodecyl sulfate (SDS), 5 mM ethylenediaminetetraacetic acid (EDTA), and 200 mM NaCl] containing 0.5 mg/mL proteinase K overnight (>16 h) at 55°C. To extract the DNA, samples were incubated for 30 min at room temperature with phenol/chloroform. After centrifugation, the soluble fraction was transferred to a new tube and DNA was precipitated with 100% ethanol. DNA was washed with 70% ethanol and finally dissolved in distilled/deionized autoclaved water. Mice-tail DNA was used to perform the polymerase chain reaction (PCR) for leptin receptors. Primer sequences: 5' AGA ACG GAC ACT CTT TGA AGT CTC 3' and 5' CAT TCA AAC CAT AGT TTA GGT TTG TGT 3' (Jackson Laboratory) at 52°C. PCR products were digested with *Rsa I* restriction enzyme. *Rsa I* recognizes the leptin-receptor point mutation; 2% low-melting agarose gel was used to separate the bands to identify wild-type, heterozygous, and homozygous leptin-receptor mice.

3T3-L1 co-culture

PancO2 cells were co-cultured with 3T3-L1 adipocytes. 3T3-L1 cells were cultured and differentiated to adipocytes in the Boyden chamber wells. PancO2 cells were seeded in the membrane and co-cultured with mature adipocytes for 72 h under the treatment of metformin. PancO2 and adipocyte cells were trypsinized and counted. Adipocytes were used to normalize based on the cell number. One-way ANOVA statistical analysis was used. Error bars represent 95% confidence intervals.

Lentiviral infection

FG12 plasmid and virus-packaging constructs were kindly provided by Dr Paul Chiao. The FG12 plasmid contains the luciferase promoter, hereafter called Luc-FG12. Packaging vectors contain the expression plasmid lentiviral vector vesicular

stomatitis virus (VSV)-G and two human immunodeficiency virus (HIV) lentiviral packaging constructs pRSVREV and pMDLg/pRRE [20]. To produce the virus, 293 T-cells were transfected with 10 µg of each plasmid Luc-FG12 [containing green fluorescent protein (GFP) and luciferase], VSV-G, pRSVREV, and pMDLg/pRRE using liposomes [21]. Virus was collected 48 and 72 h after transfection of 293 T-cells. Culture medium from 293 T-cells was collected and filtered using a 45-µm syringe filter. Then, 2 mL of fresh media and 8 µg/mL of polybrene were added to the media containing the virus. Virus-containing medium was used to infect PancO2 cells, which were plated the day of the transfection into six-well plates. After adding 2 mL of virus-containing media to each well, the cell plate was centrifuged at 1,800 rpm for 45 min. Plates were incubated at 37°C and 5% CO₂. Infection was repeated at 48 and 72 h. To confirm transfection, the cells could be observed under the microscope to detect the GFP. To select only those infected cells positive for GFP, flow-cytometry analysis cell sorting was performed. Sorted cells were expanded and used for mice experiments.

Pancreatic cancer orthotopic syngeneic mouse model

Mouse treatment with metformin started 2 weeks prior to the surgery. Metformin was provided by oral gavage increasing doses starting from 50 mg/kg/day up to 300 mg/kg/day for *Lepr^{db/db}* mice. The mice were prepared for surgery by shaving the left side of their bodies prior to the surgery. Isoflurane (Fisher) was used to anesthetize the mice to perform the surgery; 200,000 PancO2 cells were prepared by mixing with 30 µL matrigel (BD Bioscience) and were injected into the pancreas of the mice.

Oral glucose-tolerance test (OGTT)

Mouse glycemic status was established by OGTT [22]. Mice were fasted for 16 h prior to the OGTT and blood glucose was measured. Mice were glucose orally gavaged (1.5 g/kg) and OGTT was measured at time points of 15, 30, 60, and 120 min.

In vivo imaging

Tumor growth was monitored using a Xenogen IVIS 100 (Perkin Elmer; Waltham, MA, USA). We used 150 mg/kg D-luciferin (Perkin Elmer) intraperitoneal-injected into each mouse prior to the imaging. Images were captured at 5-, 10-, and 15-min time points after D-luciferin injection.

Multiplex analysis

Protein samples from allografted PancO2 tumors were used for multiplex immuno-analysis (EMD Millipore; Billerica, MA, USA) to study the AKT/mTOR pathway as previously described [14]. Total and phosphorylated proteins were analysed. Multiplex employs a unique combination of a magnetic microsphere covalently coupled to the antibody to capture the protein of interest. A second biotinylated labeled antibody detected the protein of interest in a secondary site to make an immuno-sandwich. These combinations of dyes generated a unique fluorescent signature for each bead set. Multiplex was performed in 96-well plates using approximately 20 µg of protein per kit to detect several target proteins in each sample. Magnetic beads were maintained in the bottom of the plate using a magnet for at least 1 min before changing the different buffers and solutions. Streptavidin-phycoerythrin (SA-PE) was used for detection. The Luminex 200 system (Luminex Corporation; Austin, TX, USA) was used to analyse the samples.

Transcriptomic analysis

A portion of the orthotopic syngeneic pancreatic cancer tumors obtained at the end point was used for total RNA extraction with TRIzol (Life Science Technologies). Gene-expression analyses of the RNA samples were performed at the Genomic Core Facility at the University of Texas MD Anderson Cancer Center. An Illumina MouseWG-6_V2_0_R3 (Illumina Inc., Madison, WI, USA) array platform was used to examine the transcriptomic profile of the allografted PancO2 pancreatic tumor samples. Data obtained from the gene array were analysed using Nexus Expression Analysis (BioDiscovery Inc., Hawthorne, CA, USA). Those genes that were found to have a significant difference ($P < 0.01$) were further analysed. Genes with changed expression that was significant ($P \leq 0.01$, absolute value of log ratio > 0.1 , pool size for intensity-based pooling 100,000) are presented as heat maps and also are listed in the tables.

Metabolic analysis

Pancreatic tumors were collected from mice and were snapped frozen for metabolomic analyses (Metabolon; Durham, NC, USA). Eight samples of each group of control (lean), diabetic (*Lepr^{db/db}*), and *Lepr^{db/db}* mice treated with metformin were collected. Samples were processed for Metabolon standard solvent extraction method. Then, samples were divided into two parts for gas chromatography/mass spectrometry (GC/MS) and liquid chromatography/MS/MS (LC/MS/MS). For pair-wise tests, Welch's t-test and/or Wilcoxon's rank-sum test were used. For repeated measurements, ANOVA analysis was used. For classification, random forest analysis was performed. Statistical analyses were performed with the program 'R', <http://cran.r-project.org/>.

Statistical analysis

Sigma plot software (Systat Inc., San Jose, CA, USA) or GraphPad Prism version 6 was utilized to perform the statistical analyses. Different tests were used during this project according to the experimental design. Student's t-test or one-way ANOVA was used to establish statistical differences. Statistical difference was considered if $P \leq 0.05$.

Results

Role of metformin in regulating pancreatic cancer cell growth, migration, and glucose uptakes

High levels of glucose and insulin are some of the characteristics of DM2. Therefore, we studied the effect of glucose and insulin on pancreatic cancer cell growth. Pancreatic cancer cells, MIA PaCa-2, were initially plated at an equal number with different concentrations of insulin and glucose to mimic DM2 and cultured for 72 h. Live cells were measured by MTT assay measuring the optical density at 570 nm (Figure 1A). The data indicate that DM2 promotes pancreatic cancer cell growth.

As the diabetic condition promotes pancreatic cancer cell growth, we hypothesize that controlling glucose levels may be beneficial. MIA PaCa-2 cells were cultured with different anti-diabetic treatments (metformin, rosiglitazone, and exenatide) and the anti-obesity treatment (orlistat). Results show that metformin, rosiglitazone, and orlistat decrease the pancreatic cancer cell proliferation under normal and diabetic conditions (Figure 1B). We also showed that metformin and rosiglitazone prevent pancreatic cancer cell migration as demonstrated in

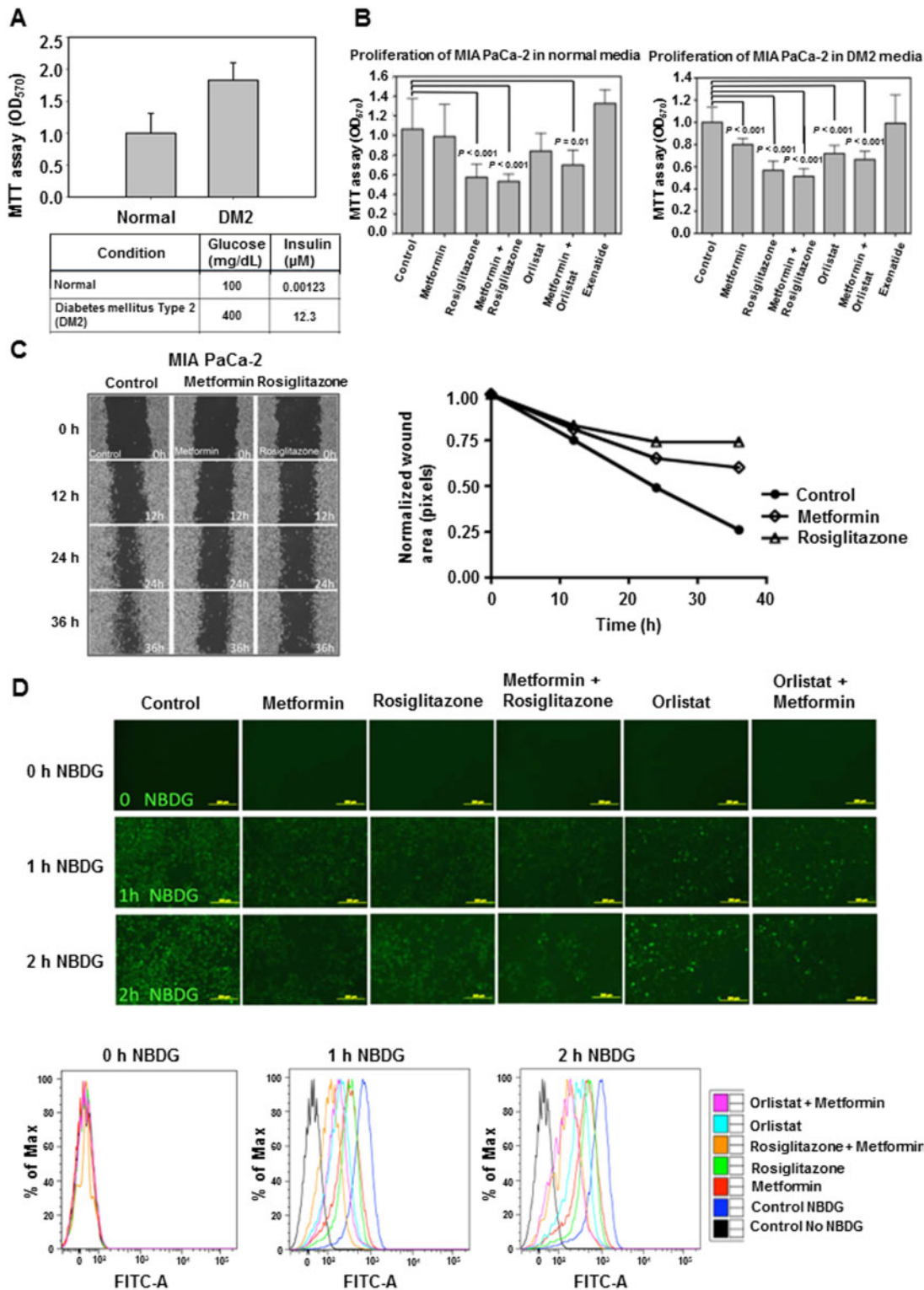


Figure 1. Metformin and rosiglitazone suppress cancer cell growth, migration, and glucose uptakes. (A) Diabetes mellitus type 2 (DM2) media enhance pancreatic cancer cells proliferation. MIA PaCa-2 cells were cultured for 72 h in conditioned medium for DM2. Statistical analysis shows significant differences between normal-condition media and DM2 media. (B) MIA PaCa-2 proliferation is reduced by metformin, rosiglitazone, and orlistat treatments. MIA PaCa-2 cells control or treated with metformin (20 mM), rosiglitazone (100 μ M), orlistat (10 mM), and exenatide (250 μ g/mL). Cells were cultured for 48 h with the treatments in normal or DM2 conditioned medium as indicated. MTT assays were performed and plotted. Error bars are 95% confidence intervals. (C) Metformin and rosiglitazone inhibit the migration of MIA PaCa-2 cells. MIA PaCa-2 cells were plated and incubated to form a monolayer. Then, a wound (scratch) was made and treatments were added. Wound closure was monitored using time-lapse microscopy and images of MIA PaCa-2 cells show the wound area over different time points of 0, 12, 24, and 36 h (left). Plot of the quantitated wound area at different time points. Each treatment was normalized with its time 0 h (initial wound area) (right). (D) Metformin, rosiglitazone, and orlistat reduce glucose uptake in pancreatic cancer cells. Representative fluorescent images of MIA PaCa-2 cells taken at 0, 1, and 2 h of 2-NBDG incubation for control or treatments, metformin, rosiglitazone, metformin + rosiglitazone, orlistat, and orlistat + metformin (top panel). Flow-cytometry analysis showing 2-NBDG uptake (bottom panel).

wound-healing assays (Figure 1C). The wound gap was narrower after 36 h in the control while the wounds of cells with metformin and rosiglitazone treatments remained open (Figure 1C). The wound area was measured and plotted (Figure 1C), and both treatments prevented wound closure, indicating a reduction in cell migration.

The DM2 condition promotes cell growth, which is probably due to the high glucose uptake of the cells. As anti-diabetic drugs can suppress cell growth, we hypothesize that anti-diabetic drugs (metformin and rosiglitazone) and the anti-obesity drug (orlistat) may have an impact on glucose uptake. 2-NBDG, a fluorescent glucose analog (Life Science Technologies), was used in glucose-uptake experiments. Cells that had glucose uptake were seen as fluorescent (Figure 1D). In addition, flow-cytometry analysis was performed to quantitate the number of cells positive for 2-NBDG (Figure 1D). All the treatments showed reduced glucose uptake when compared with control, non-treated cells. Together, some of the anti-diabetes drugs are potent in affecting cell growth, migration, and glucose uptakes.

Metformin impacts on cancer-energy metabolism to suppress tumor growth in a pancreatic cancer xenograft model

We proceeded to measure the basal ECAR in cells treated with metformin to understand the glycolytic flux. ECAR was lower in the metformin-treated when compared with non-treated control cells. OCR, indicative of mitochondrial respiration, was also lower in the metformin-treated cells (Figure 2A).

To test the potential for metformin and rosiglitazone to inhibit the growth of pancreatic cancer *in vivo*, a nude-mice xenograft mouse model was used. Mice were subcutaneously injected with MIA PaCa-2 cells in the flanks. Metformin or rosiglitazone treatments were provided in the drinking water starting on the day of the injection. Twenty-five days after injection, mice were sacrificed by CO₂ asphyxiation followed by cervical dislocation. Representative mice and tumors from control, rosiglitazone, and metformin treatment are shown (Figure 2B). Mice tumors were excised and weighed. The tumor weight was plotted against each treatment (Figure 2B). Rosiglitazone and metformin both show a decrease in the tumor weight, but metformin was the one with the largest change. Also, staining of Ki-67 in these metformin-treated tumor samples showed a decrease in staining when compared with the control (Figure 2C). In addition, cleaved caspase-3 staining was increased in the indicated treated groups (Figure 2C).

Metformin suppresses tumor growth in an orthotopic/syngeneic pancreatic cancer model under diabetic conditions

In order to further understand the impact of DM2 in pancreatic cancer, we employed diabetic orthotopic/syngeneic allograft mouse models. We selected PancO2-Luc-FG12 cells to construct the orthotopic pancreatic cancer model. To mimic the potential conditions in the diabetic-mouse system, we used the *in vitro* co-culture system to grow PancO2 cells (B6 background, mouse origin) with 3T3-L1 differentiated adipocytes. After 72 h of treatment with metformin, our results showed that metformin significantly decreases adipocytes-induced pancreatic cancer cell proliferation at concentrations of 0.5 and 1 mM (Figure 3A).

The scheme of constructing the orthotopic/syngeneic PancO2-Luc-FG12 pancreatic cancer model is illustrated (Figure 3B). We

used *in vivo* tumor bioluminescence imaging from allografted PancO2-Luc-FG12 tumors to access the effect of DM2 on pancreatic tumor growth. Pancreas of *Lepr^{db/db}* in a CB57 BL/6 background can be injected with PancO2-luc-FG12 cells for constructing the orthotopic pancreatic cancer model. OGTT was performed to confirm the glucose-tolerance status of the newly constructed model with allografted PancO2-Luc-FG12. Our diabetic-mouse (*Lepr^{db/db}*) model allografted with PancO2-Luc-FG12 demonstrated severe glucose intolerance (Figure 3C). In addition, we showed that the glucose intolerance of these diabetic-mouse models was ameliorated by 2-week treatment with metformin (300 mg/kg/day) (*Lepr^{db/db}*) (Figure 3C).

Weekly bioluminescence imaging of the orthotopic/syngeneic PancO2-luc-FG12 pancreatic cancer model was performed to monitor the tumor growth. Our results show that diabetic (*Lepr^{db/db}*) allografted-tumor growth is significantly accelerated when compared with the lean control group (Figure 4A). Significantly, metformin-treated diabetic (*Lepr^{db/db}*) allografted tumors demonstrated decelerated tumor growth when compared with the non-metformin-treated group (Figure 4A).

Protein and phospho-protein level analyses of these allografted tumors revealed that the DM2 condition induces activation of AKT/mTOR signaling pathway members as assayed by multiplex (Figure 4B). We found that treatment with metformin can revert this impact (Figure 4B). Allografted pancreatic cancer tumors from these models were analysed for gene-expression profiles. Using gene set enrichment analysis (GSEA) [23] as previously described [24], we showed a significant upregulation of the protein kinase B (AKT) target genes, glucose metabolism genes, and epithelial-mesenchymal transition (EMT) genes in (*Lepr^{db/db}*)-allografted tumors (Figure 4C). Again, treatment with metformin can revert these profiles of (*Lepr^{db/db}*)-allografted tumors.

Metformin treatment changes the transcriptomic landscape in orthotopic/syngeneic pancreatic tumor allografts

The allografted PancO2-luc-FG12 pancreatic cancer tumors from diabetic mice had a significantly increased expression of 2,078 genes and significantly decreased expression of 3,937 genes compared with those from non-diabetic lean littermate mice (Figure 5). Metformin-treated diabetic mice had a significantly increased expression of 218 genes and significantly decreased expression of 172 genes compared with those from non-treated diabetic mice (Figure 5). We used Nexus Expression 3 software to perform unsupervised functional transcriptomic analysis. This analysis identified 18 biological processes that were significantly different ($P < 0.01$) between DM2 and non-diabetic mice (Table 1). We also identified 76 biological processes between the metformin-treated diabetic and non-treated diabetic mice (Table 2). Thus, our data suggest that the diabetic *in vivo* environment promotes tumor growth and aggressiveness via activating the AKT/mTOR signaling pathway, inducing transcriptional changes in the glucose metabolism and fostering a more invasive phenotype. Significantly, metformin can change the transcriptomic landscape to suppress cancer growth.

Metformin treatment leads to metabolomic changes in orthotopic/syngeneic pancreatic tumors

In order to investigate the metabolomic changes induced by diabetes, we used the PancO2-luc-FG12 allografted

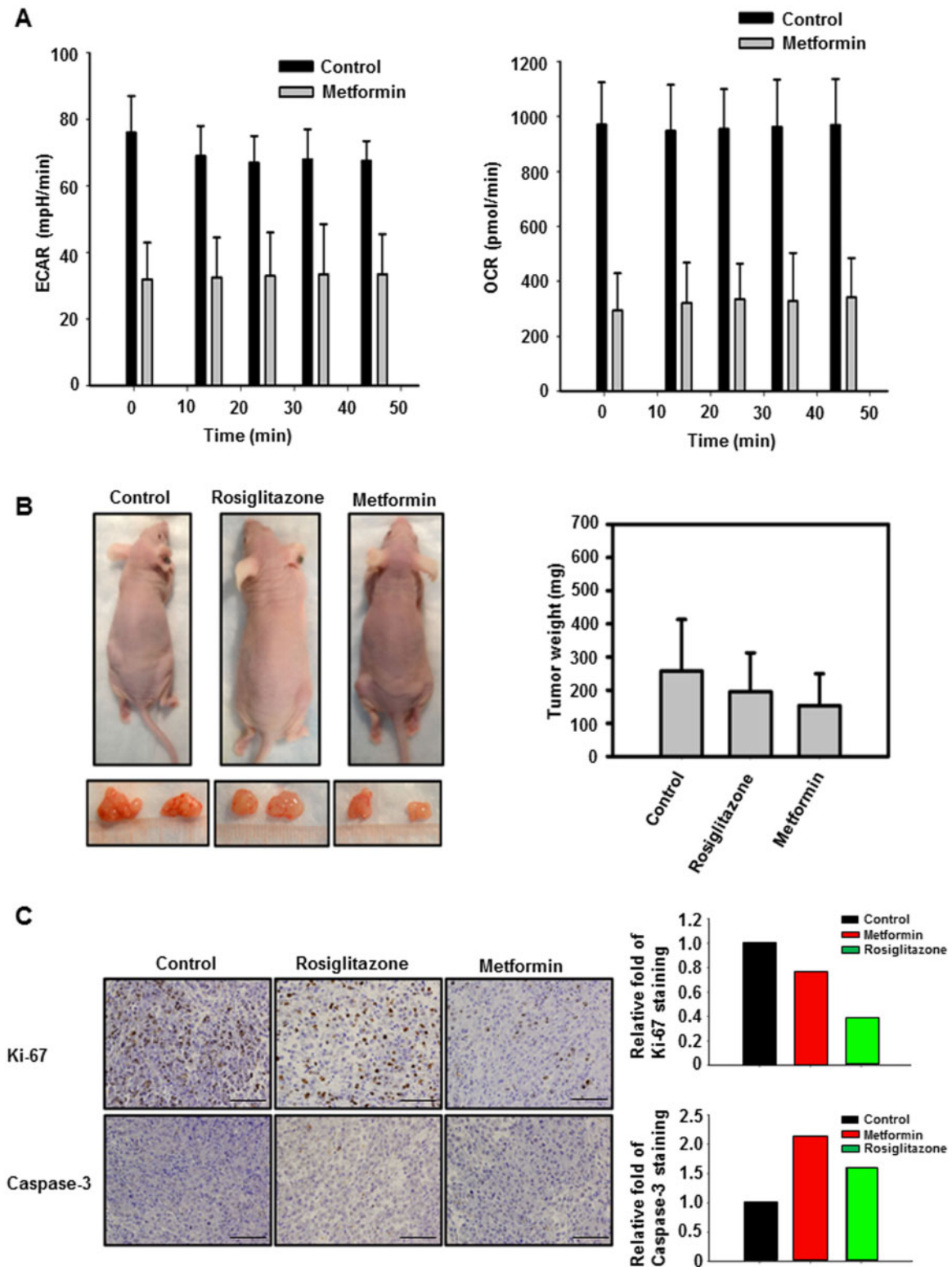


Figure 2. Metformin and rosiglitazone promote energy reprogramming of pancreatic cancer cells and suppress tumor growth in a pancreatic cancer xenograft model. (A) Extracellular acidification rates (ECARs) and oxygen-consumption rates (OCRs) were measured in MIA PaCa-2 tumor cells treated with 5 mM metformin and untreated controls. Tumor cells were seeded into a 96-well plate for analysis. Values are means \pm standard deviation. (B) MIA PaCa-2 pancreatic cancer xenograft model. Representative mice from control, rosiglitazone-treated, metformin-treated, and their resected tumors. Tumor-weight difference is demonstrated. (C) Immunohistochemistry (IHC) analysis of MIA PaCa-2 tumor xenograft after the indicated treatments. Tumors from xenografts were analysed by IHC. Scale bars represent 50 μ m. Amounts of Ki-67 and cleaved caspase-3 staining were quantitated.

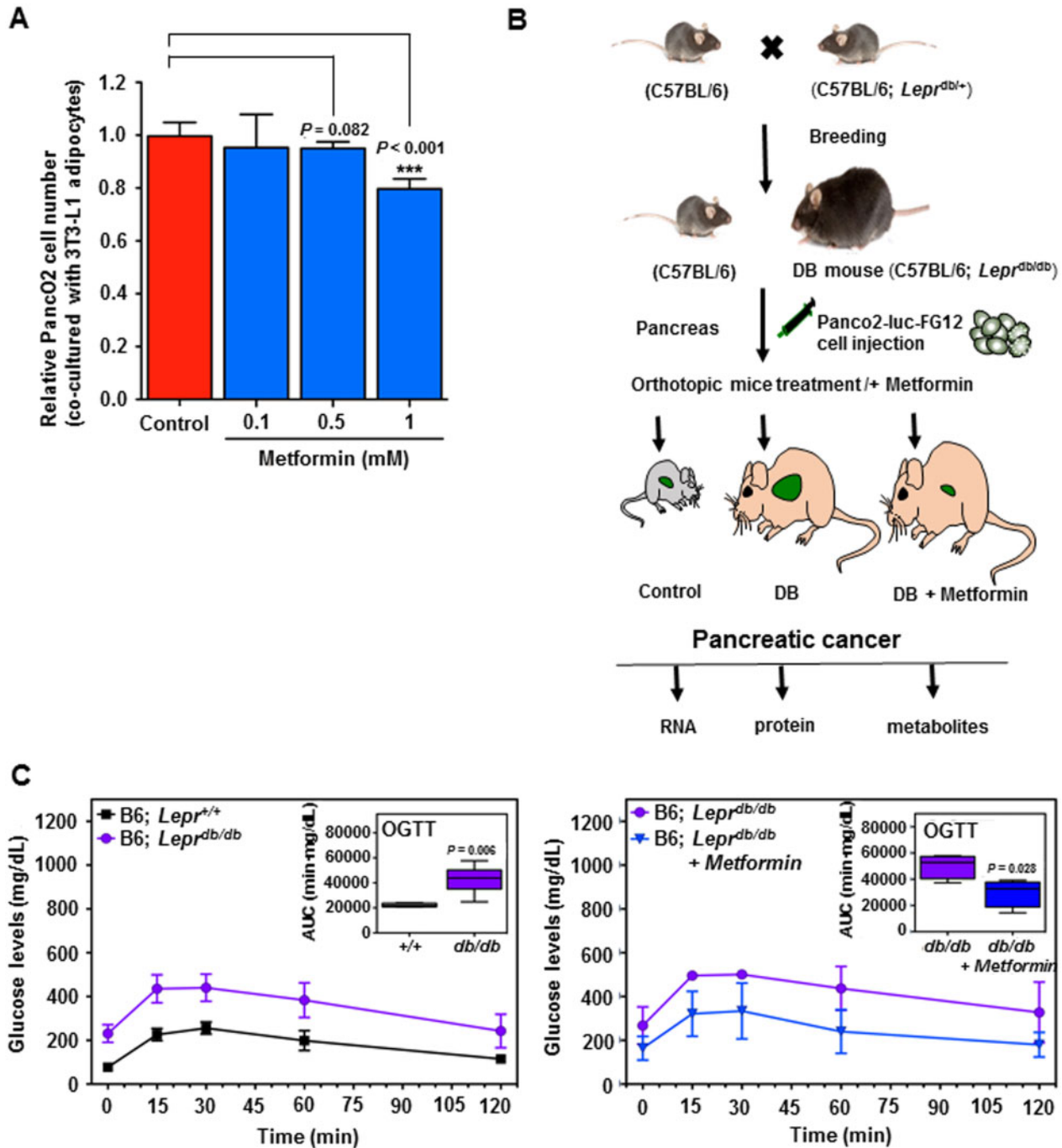


Figure 3. Constructing an orthotopic/syngeneic pancreatic cancer model under diabetic conditions. (A) Metformin reduced the proliferation of PancO2 co-cultured with 3T3-L1 adipocytes. A Boyden chamber co-culture system (0.4 μ m membrane) was used to determine the effect of metformin in PancO2 proliferation when co-cultured with 3T3-L1. An equal number of PancO2 cells were co-cultured with differentiated 3T3-L1 adipocytes treated with control (no treatment), 0.1 mM metformin, 0.5 mM metformin, and 1 mM metformin for 72 h. The graph shows the proliferation of PancO2 cells normalized with the number of adipocytes. One-way ANOVA statistical analysis was used to compare the groups. Error bars represent 95% confidence intervals. (B) Scheme of mouse breeding of the orthotopic/syngeneic PancO2-luc-FG12 pancreatic cancer model. Mice (C57BL/6) were crossed with *Lepr*^{db/db} mice (C57BL/6) to breed the C57BL/6 and *Lepr*^{db/db} in a C57BL/6 background. The pancreases of indicated mice were injected with PancO2-luc-FG12 cells for constructing an orthotopic pancreatic cancer model. Tumor samples were used for analysing the difference in the metabolites, gene expression, and protein levels. (C) Metformin decreased the diabetes-induced glucose intolerance in diabetic orthotopic/syngeneic pancreatic cancer mouse model. Oral glucose-tolerance tests (OGTT) of diabetic (B6; *Lepr*^{db/db}, n = 10) and lean (B6; *Lepr*^{+/+}, n = 4) littermate mice. Error bars represent 95% confidence intervals (left). OGTT of diabetic (B6; *Lepr*^{db/db}, n = 4) and metformin-treated (300 mg/kg/day) diabetic mice (B6; *Lepr*^{db/db} + Metformin, n = 4) after 2 weeks of treatment (right). Error bars represent 95% confidence intervals.

pancreatic tumor samples to perform metabolomic analysis. Global biochemical profiling of allografted-tumor tissues revealed a large number of differences that were observed in

diabetic mouse models, as compared with control littermates. Metabolomic results showed that 117 metabolites are significantly different between the DM2 and non-diabetic mice. Most

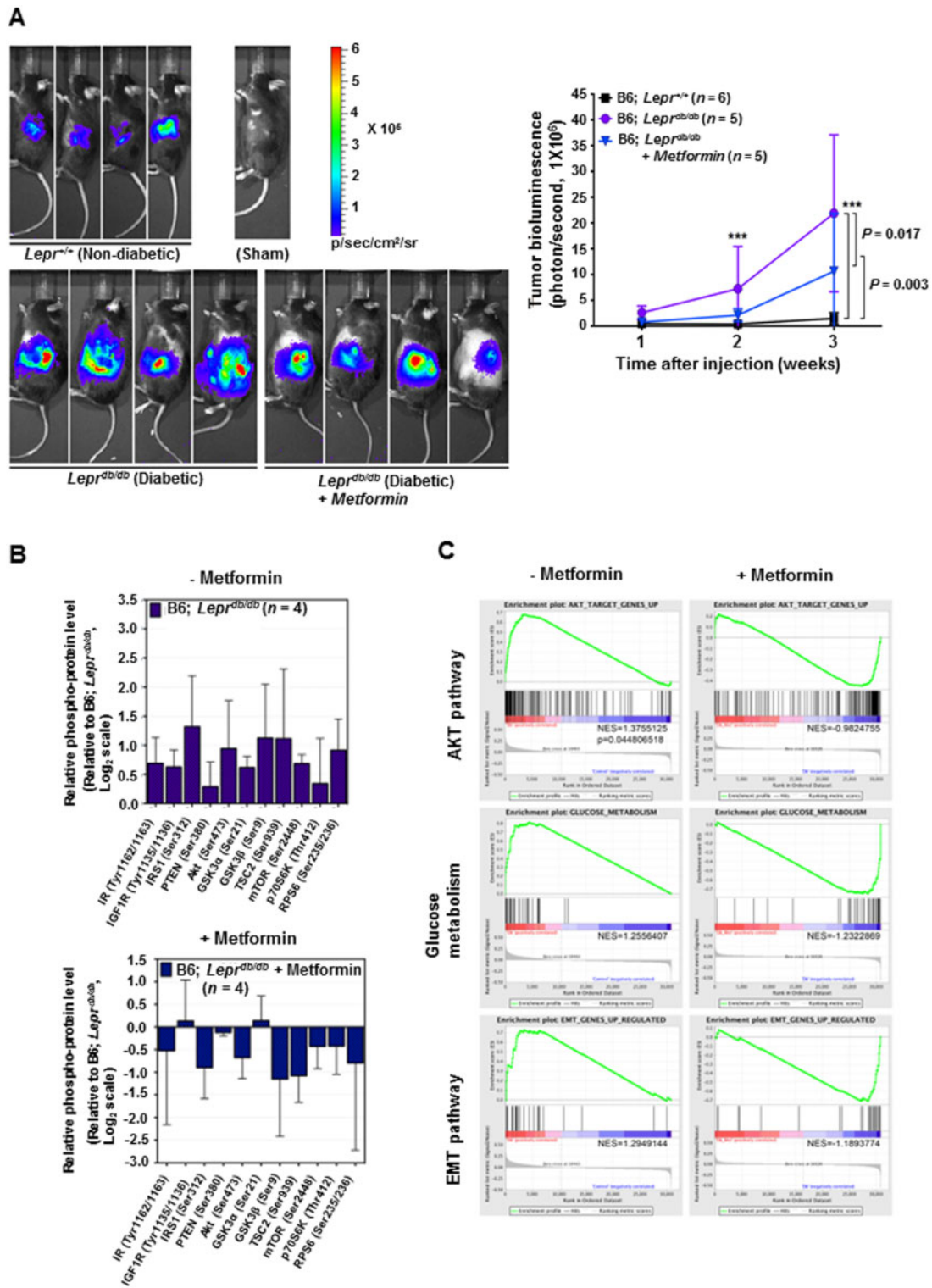


Figure 4. Metformin and rosiglitazone suppress the tumor growth of diabetes-induced orthotopic/syngeneic pancreatic tumors. (A) Metformin decreases diabetes-induced orthotopic/syngeneic pancreatic tumor (PancO2-luc-FG12) allograft growth. Representative *in vivo* imaging of the bioluminescence of tumors performed 3 weeks after orthotopic/syngeneic injection. Line graph of the relative bioluminescence intensity generated by the tumor of randomized B6; *Lepr*^{-/-} (lean, *n* = 6), B6; *Lepr*^{db/db} (diabetic, *n* = 5), and metformin-treated B6; *Lepr*^{db/db} (*n* = 5) mice injected into the pancreas body with pancreatic cancer (syngeneic PancO2-luc-FG12) after treatment. Error bars represent 95% confidence intervals (right). (B) Multiplex analysis of the protein mediators of the signaling pathways in tumors of the indicated pancreatic cancer model. Syngeneic PancO2-luc-FG12 tumors were harvested from untreated diabetic *Lepr*^{db/db} mice (*n* = 4) and from those diabetic *Lepr*^{db/db} mice treated with metformin (*n* = 4). Tumor-cell lysates were prepared for multiplex analysis. (C) Gene Set Enrichment Analysis (GSEA) of transcriptomic profile generated from tumors in non-treated diabetic *Lepr*^{db/db} mice and metformin-treated diabetic *Lepr*^{db/db} mice are demonstrated. GSEA are presented for AKT activation target genes (top), genes involved in the glucose metabolism (middle), and genes involved in the epithelial–mesenchymal transition (EMT) and metastasis (bottom). Each bar corresponds to one gene.

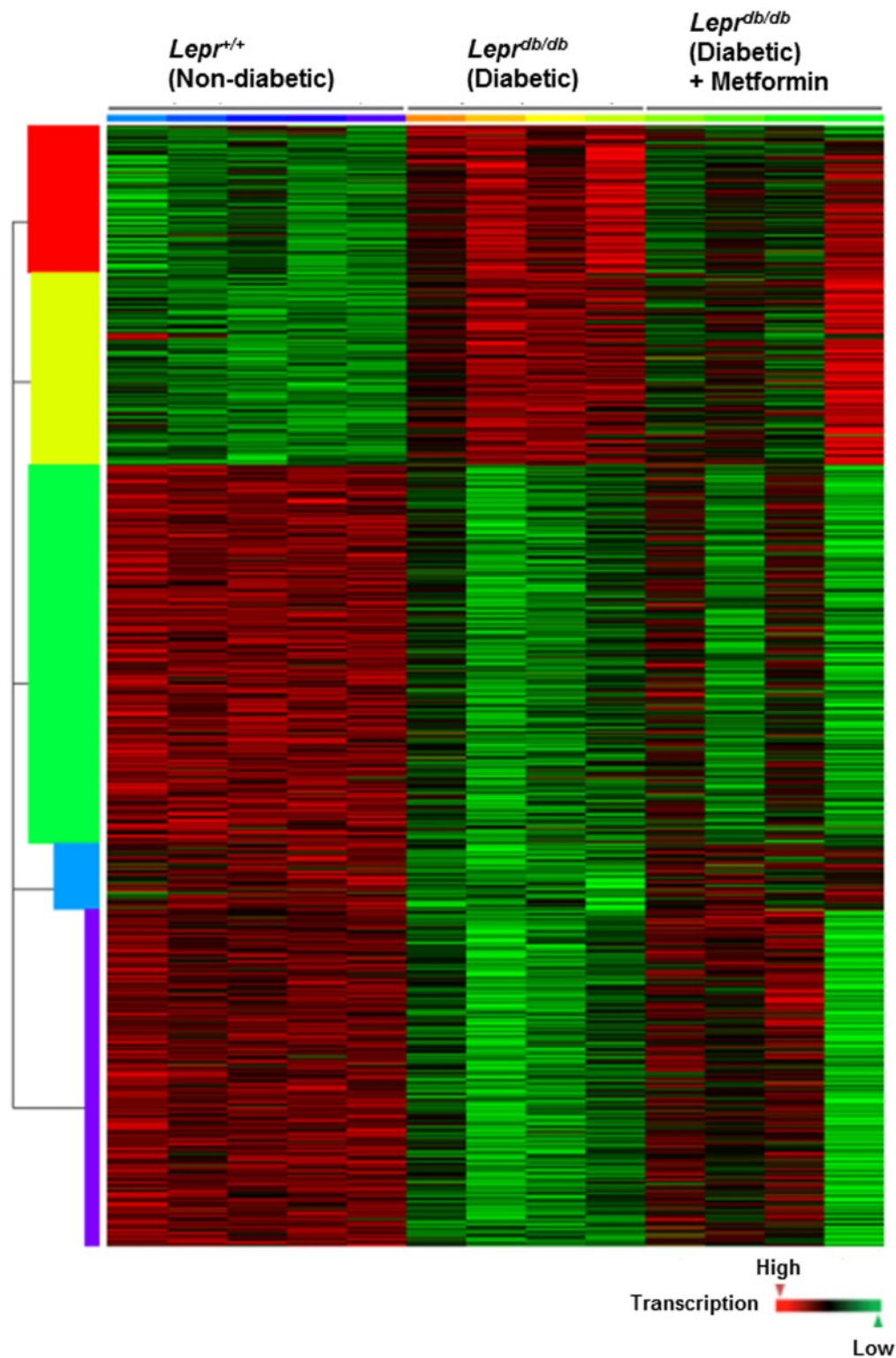


Figure 5. Metformin treatment changes the transcriptomic landscape in orthotopic/syngeneic pancreatic tumor allografts. Heat map of the gene expression significantly changed ($P \leq 0.01$, absolute value of log ratio > 0.1 , pool size for intensity-based pooling 100,000; identified by Nexus Expression software) in PancO2-luc-FG12 pancreatic tumor allografts from diabetic mice (B6; *Lepr*^{db/db}, $n = 4$) and metformin-treated diabetic mice (B6; *Lepr*^{db/db} + Metformin, $n = 4$) relative to those from non-diabetic lean littermate mice (B6; *Lepr*^{+/+}, $n = 5$).

of these differences are associated with lipid metabolism, amino acids, dipeptides, nucleotides metabolism, and oxidative stress. Metformin treatment in PancO2-luc-FG12 pancreatic

tumor allografts from diabetic mice (B6; *Lepr*^{db/db}) leads to changes in the profile of metabolites when compared with the non-metformin-treatment controls (Figure 6A).

Table 1. Biological processes significantly ($P < 0.05$) changed in orthotopic/syngeneic PancO2-luc-FG12 pancreatic tumor allografts from diabetic compared with non-diabetic mice identified by Nexus Expression

Biological process	Score	P-value
Actin cytoskeleton organization and biogenesis	1.477698164	0.016483516
Gamma-aminobutyric acid-signaling pathway	-1.689808152	0.017509728
Cell redox homeostasis	1.498312572	0.017509728
Protein-chromophore linkage	-1.543916303	0.01863354
Phosphorylation	1.529232379	0.01875
Tricarboxylic-acid cycle	1.570427574	0.018907563
Mo-molybdopterin cofactor biosynthesis	1.450729032	0.031936128
Ubiquitin-dependent protein catabolism	1.458953173	0.034615385
Purine nucleotide biosynthesis	1.599643861	0.036538462
Proton transport	1.41897114	0.037280702
Axon guidance	-1.418488144	0.03815261
Protein homotetramerization	1.382782216	0.040152964
Cell motility	1.521752194	0.042635659
Cobalt ion transport	-1.454758732	0.045833333
Ovulation (sensu Mammalia)	-1.570571153	0.04743083
Tetrahydrobiopterin biosynthesis	1.523609736	0.048300537
Copper-ion transport	1.49906061	0.049212598
Calcium-dependent cell-cell adhesion	-1.391442349	0.049242424

Tumors from diabetic mice showed significantly low levels of metabolites of the kynurenine pathway (KP), including tryptophan, kynurenine (KYN), and nicotinamide adenine dinucleotide (NAD⁺), when compared with lean controls (Figure 6B). Tryptophan is metabolized through two pathways: KP and serotonin/melatonin pathway. The KP regulates L-tryptophan (Trp) catabolism through the production of KYN, kynurenic acid, picolinic acid (PIC), quinolinic acid (QA), the essential pyridine nucleotide, and NAD⁺. NAD⁺ is a coenzyme-regulating electron transferred during oxidation-reduction reactions and is involved in various physiological processes, including metabolism, aging, post-translational protein modification, and DNA repair [25]. Interestingly, PancO2-luc-FG12 pancreatic tumor allografts from diabetic mice (B6; *Lepr^{db/db}*) treated with metformin demonstrated elevation of these metabolites, suggesting that metformin regulates KP.

In addition, levels of taurine (2-aminoethanesulfonic acid) and choline were significantly lower in allografted tumors from diabetic-mouse models relative to control littermates. Taurine is a sulfur-containing amino acid that has a cholesterol-lowering effect [26]. It is involved in a plethora of physiological functions, such as bile salt conjugation, osmoregulation, membrane stabilization, calcium modulation, anti-oxidation, and anti-inflammation. As for choline, choline is a conditional vitamin [27] and severe choline deficiency instigates DNA-strand breaks in rodents, causing alterations to epigenetic markers and impacts on brain development. Again, PancO2-luc-FG12 pancreatic tumor allografts from diabetic mice (B6; *Lepr^{db/db}*) under metformin treatment caused the elevation of taurine and choline metabolites (Figure 6C and D), indicating that metformin regulates these metabolites to modulate the metabolite profile of pancreatic cancer affected by DM2.

Discussion

Metabolic alterations are necessary to support the uncontrolled growth of tumor cells. Although characteristics of the DM2 such as hyperglycemia, hyperinsulinemia, and high circulating insulin-like growth factors may contribute to the metabolic changes and proliferation of pancreatic cancer cells, the details of metabolite changes remain poorly characterized. Here, we showed the effects of metformin on pancreatic cancer cell metabolism in the context of DM2. Metformin is identified as a glucose-uptake regulator and has impacts on AKT signaling, glucose metabolism, and the EMT pathway. Notably, we evaluated the effect of metformin in orthotopic/syngeneic PancO2-luc-FG12 pancreatic cancer animal models under DM2 condition and showed that metformin alters the metabolic reprogramming of pancreatic cancer in the presence of DM2 to suppress cancer growth. This study provides insights into the metabolic regulatory circuit of pancreatic cancer under DM2 and elucidates how metformin signals in interfering with this metabolic rewiring to hinder cancer development.

We have found that some anti-diabetic treatments, particularly metformin, may be beneficial for the treatment of pancreatic cancer under DM2 conditions. It is worthwhile to mention that, in addition to metformin, other treatments (rosiglitazone, orlistat) seem to have a beneficial impact on preventing pancreatic cancer cell proliferation. For example, we tested the effect of metformin, rosiglitazone, and orlistat on glucose uptake and found that all of them reduced the glucose uptake in the MIA PaCa-2 cells. This result could be indicative of a switch in metabolism caused by these drugs. As has been defined by Otto Warburg, cancer cells rely on glycolysis [28, 29]. Our results indicate that metformin and rosiglitazone affect the glucose uptake to interfere with the growth advantage (Warburg Effect) of the cancer cells. Although rosiglitazone has been withdrawn from the market because of its cardiotoxic effects, the use of pioglitazone, another thiazolidinediones drug, may be useful for the treatment of pancreatic cancer patients with DM2 condition. Orlistat was approved by the FDA (Alli) to use for weight loss. Based on its impact on glucose uptake in our *in vitro* results, it may be a promising treatment for the adjuvant treatment of cancer patients, especially for obese or diabetic patients. In terms of exenatide, we did not observe any effect in the *in vitro* experiments, but it is possible that *in vivo* use will have a different outcome. Further studies to explore these other anti-diabetic drugs in treating pancreatic cancer under DM2 conditions warrant further exploration.

Our orthotopic/syngeneic PancO2-luc-FG12 pancreatic cancer animal models (Figure 3) recapitulated the increased caloric intake that eventually promotes the development of diabetes in humans. In this way, we were able to study the diabetic-related biological changes that promote pancreatic tumor growth and overall pancreatic cancer aggressiveness. Importantly, we integrated high-throughput screening (e.g. transcriptomics and metabolomics) of tumors from our orthotopic/syngeneic PancO2-luc-FG12 pancreatic cancer animal models to explore the biological mechanisms involved in DM2-accelerated pancreatic cancer. However, more investigation is required to further confirm these regulatory mechanisms. Our animal model is a unique strategy to unveil the impact of diabetes on pancreatic cancer growth and is a tool to better dissect the tumor-suppressing effect of anti-diabetic drugs. First, our orthotopic/syngeneic PancO2-luc-FG12 pancreatic cancer animal models provided strong evidence for the causal relationship between diabetes and accelerated pancreatic cancers. Second, we

Table 2. Biological processes significantly ($P < 0.05$) changed in orthotopic/syngeneic PancO2-luc-FG12 pancreatic tumor allografts from metformin-treated diabetic compared with non-treated diabetic mice identified by Nexus Expression

Biological process	Score	P-value
Cytoskeleton organization and biogenesis	-1.474161038	0.021543986
Microtubule-based movement	-1.393981536	0.022556391
Embryonic development (sensu Mammalia)	-1.370492704	0.02259887
Negative regulation of protein kinase activity	-1.278196419	0.02259887
Actin cytoskeleton organization and biogenesis	-1.374793819	0.022944551
Innate immune response	1.59139184	0.023076923
Nitrogen compound metabolism	-1.577897779	0.023121387
Axon guidance	1.836990889	0.023166023
Fatty-acid desaturation	-1.682510548	0.023210832
Negative regulation of cell differentiation	-1.639949091	0.023210832
Negative regulation of myeloid cell differentiation	-1.454776683	0.023255814
Cell glucose homeostasis	2.028564801	0.023300971
Protein polymerization	-1.683135887	0.023300971
Transcription initiation	1.432132918	0.023300971
Negative regulation of fibroblast proliferation	-1.429501064	0.023575639
Regulation of cholesterol absorption	-1.176428311	0.023668639
Natural-killer-cell differentiation	-1.628094531	0.023715415
Regulation of cytokine biosynthesis	-1.524173487	0.023762376
Ovulation (sensu Mammalia)	1.643051453	0.023904382
Embryonic-pattern specification	-1.648132032	0.023952096
Fatty-acid metabolism	-1.378046378	0.024
T-cell receptor signaling pathway	1.840245041	0.024048096
Proteoglycan biosynthesis	-1.409921279	0.024096386
Embryonic limb morphogenesis	-1.777445325	0.024144869
Mitotic chromosome condensation	-1.441479318	0.024144869
Melanocyte differentiation	-1.568416412	0.024291498
Excretion	1.479631366	0.024439919
Embryonic cleavage	1.590083363	0.024489796
Frizzled-2 signaling pathway	-1.632673267	0.024539877
Urogenital-system development	-1.608792927	0.024590164
Positive regulation of progression through mitotic cell cycle	-1.582991585	0.024590164
Calcium-independent cell-cell adhesion	-1.480983697	0.024691358
N-acetylglucosamine metabolism	1.603911761	0.024742268
One-carbon compound metabolism	-1.478395123	0.025052192
Defense response	1.549819808	0.025477707
Cartilage condensation	-1.474291437	0.025586354
Retrograde axon cargo transport	1.505437065	0.025641026
Immune response	1.644866022	0.026548673
Inner-ear morphogenesis	1.393060666	0.035643564
Sulfate transport	1.595707293	0.04494382
Melanin biosynthesis from tyrosine	1.559171666	0.045634921
Lipid metabolism	-1.35343213	0.046678636
Sexual reproduction	1.36838016	0.047244094
MAPKKK cascade	-1.270455816	0.048689139
Nerve growth factor receptor signaling pathway	-1.490130948	0.048828125
Organic anion transport	1.377971903	0.049701789

confirmed that the anti-diabetic drug metformin can suppress the growth of pancreatic cancer in these models, implying that the efficacy of other anti-diabetic drugs can also be explored in this animal model. Although other mouse models of DM2 can be considered, *Lepr^{db/db}* is the most appropriate animal model of DM2 for our proposed studies as they develop obesity and DM2 by the age of 2 months. The CBA Carter J strain (CBA/CaJ) develops DM2 only in males [30]; NONcNZO10/LtJ (a model of obesity and DM) is sensitive to adverse hepatic side effects of thiazolidinediones [31]. The A-ZIP/F-1 mice can be an alternative [32] but they may be less desirable because they are fatless and do not share a major contributing factor of human DM2, i.e. obesity. Together, our study sheds new insights into the effects of

metformin and its potential as part of therapeutic interventions for DM2 pancreatic cancer patients.

We found that metformin treatment in PancO2-luc-FG12 pancreatic tumor allografts from diabetic mice (B6; *Lepr^{db/db}*) results in changes in the profile of metabolites of KYN, tryptophan, taurine, and choline when compared with non-metformin-treated controls. This documents for the first time that DM2 impacts on these pathways and that metformin can suppress the tumor by correcting the metabolic deregulation of these pathways. It has been shown that KYN can cause the activation of aryl hydrocarbon receptor (AHR) to inhibit cell proliferation and promote cell differentiation [33]. KYN treatment can lead to the elevation of tumor metastasis suppressor KISS1, a

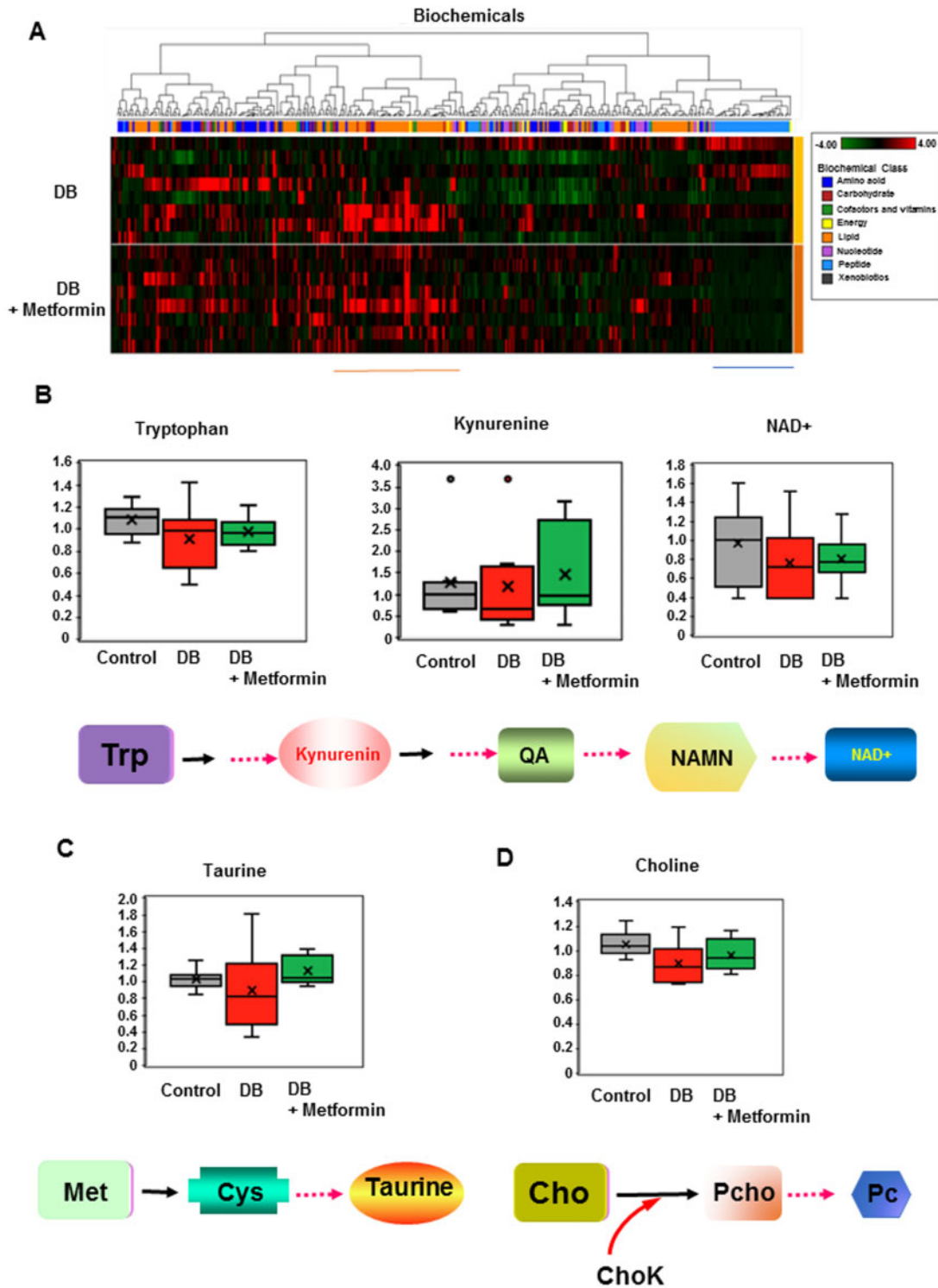


Figure 6. Metabolomic changes associated with metformin treatment in orthotopic/syngeneic pancreatic tumors. (A) Heat map of the metabolic molecules (metabolites) significantly changed ($P \leq 0.05$) in PancO2-luc-FG12 pancreatic tumor allografts from diabetic mice (B6; *Lepr^{db/db}*, $n = 8$) relative to those from metformin-treated diabetic mice (B6; *Lepr^{db/db}* + Metformin, $n = 8$). (B)–(D) Metabolites with significantly changed levels in PancO2-luc-FG12 pancreatic tumor allografts from diabetic mice (B6; *Lepr^{db/db}*, $n = 8$), metformin-treated diabetic mice (B6; *Lepr^{db/db}* + Metformin, $n = 8$) relative to those from lean littermate mice (B6 control) are indicated. The pathways involved in regulating these metabolites are shown. Trp, tryptophan; QA, quinolinic acid; NAMN, nicotinamide mononucleotide; NAD, nicotinamide adenine dinucleotide; Cho, choline; Met, methionine; Cys, cysteine; ChoK, choline kinase; Pcho, phosphocholine; Pc, phosphatidylcholine.

molecule induced by AHR, to inhibit metastasis [33]. In addition, AHR plays a role in the regulation of body mass in mice fed a Western diet [34]. So far, AHR has also been implied as a tumor

suppressor in melanoma [35] and breast cancer [36]. It has been shown that KYN regulates AHR to suppress the metastasis of neuroblastoma, possibly by enhancing cell adhesion [33]. Thus,

it is possible that metformin-mediated elevation of KYN in our pancreatic cancer model may have an impact on the suppression of tumor growth in a way similar to KYN's roles described above.

Cellular NAD levels decline with age or under disturbed nutrient conditions, including obesity, diabetes, and fatty liver disease [37]. NAD⁺ is pivotal in regulating NAD⁺-consuming enzymes, such as poly-ADP-ribose polymerases (PARPs), sirtuins, and CD38/157 ectoenzymes [38]. NAD mediates various redox reactions in glycolysis, the tricarboxylic-acid (TCA) cycle, fatty-acid oxidation, and oxidative phosphorylation, and is a substrate for sirtuins and PARPs. Therefore, it regulates many biological pathways, such as energy metabolism, cellular stress response, gene expression, and DNA repair. Nicotinamide phosphoribosyltransferase (Nampt) is a critical NAD biosynthetic enzyme, converting nicotinamide into nicotinamide mononucleotide (NAMN), an NAD intermediate. Nampt plays a role in regulating the insulin secretion of pancreatic β -cells; therefore, it has a role in DM2. Also, niacin demonstrates lipid-modifying and anti-atherosclerotic properties. It can elevate high-density lipoprotein levels [39]. Thus, metformin-mediated elevation of NAD in our pancreatic cancer model may have an impact on correcting the broad spectrum of metabolisms and DNA repair during pancreatic cancer formation. Interestingly, NAD⁺ synthesis can be met with tryptophan from the diet [40]. In other words, tryptophan is critical for NAD⁺ synthesis. The tryptophan diet can ameliorate dextran sodium sulfate-induced colitis symptoms in mouse models, suggesting that it can function as an anti-inflammation agent for ulcerative colitis [41]. Together, it is possible that metformin elevates the level of Trp, KYN, and NAD in a DM2 pancreatic cancer model to inhibit pancreatic cancer growth via regulating the above-mentioned biological activities of each metabolite.

Taurine is particularly synthesized via the cysteine sulfonic-acid pathway in the pancreas. Taurine is a longevity vitamin [27]. Plasma taurine concentrations are significantly lower in DM2 patients [42]. Taurine has excellent therapeutic potential against DM2 [43]. It can function against DM2 and insulin resistance, thereby ameliorating diabetic pathologies, such as neuropathy, retinopathy, nephropathy, cardiopathy, atherosclerosis, altered platelet aggregation, and endothelial dysfunction [44]. In addition, taurine has a cholesterol-lowering effect [26]. Taurine decreases the production of pro-inflammatory cytokines from adipocytes. At the site of inflammation, taurine can react with hypochlorous acid/hypobromous acid (HOCl/HOBr) to produce taurine haloamines (TauCl/TauBr), two less toxic milder oxidants, by the neutrophil myeloperoxidase (MPO)-halide system. Importantly, TauCl released from activated neutrophils following their apoptosis is critical to inhibit the production of inflammatory factors, including nitric oxide, tumor necrosis factor- α , interleukins, and prostaglandins [45]. As pancreatic cancer progression can develop through escaping tumor immune surveillance [46, 47], metformin's impact on the taurine-regulated immune response is critical. Further, taurine has critical functions to read alternate codons accurately in the mitochondrial genome [48]. Taurine has EMT inhibitory effects as demonstrated by the fact that taurine downregulates the expression of N-cadherin, TWIST1, ZEB1, SNAIL, and vimentin [49]. Thus, metformin increases the level of taurine to inhibit pancreatic cancer growth, possibly by functioning against DM2 and insulin resistance, regulating inflammation, and inhibiting EMT.

Choline metabolism activation is frequently observed during tumor progression. Levels of phosphocholine and glycerophosphocholine are elevated in many types of cancer [50].

Phosphocholine is involved in the biosynthesis of phosphatidylcholine (Pc), which is a major component of the phospholipid bilayer of the eukaryotic cell membrane. Molecular mechanisms involved in abnormal choline metabolism are related to changes in several regulators: including choline transporters, choline kinase- α (CHK α), ethanolamine kinase- α , phosphatidylcholine-specific phospholipase C and -D, and glycerophosphocholine phosphodiesterases [51]. It is worthwhile to mention that CHK α is oncogenic and plays a critical role in membrane phospholipid synthesis. Many cancers overexpress CHK α to increase phosphocholine, which is also increased in tumor cells. Therefore, CHK α is a cancer biomarker and can be a target for anticancer therapy [52]. We think that metformin elevates the level of choline (a conditional vitamin) to inhibit pancreatic cancer growth, possibly by targeting several choline regulators such as CHK α . However, it is important to point out that our above-mentioned metabolomic studies are based on an animal model; therefore, further investigation in much more complex human clinical situations is warranted.

In summary, our data demonstrate a link of DM2 signaling, metabolic reprogramming, and tumorigenicity. The role of metformin in attenuating the impact of DM2 on metabolism regulation during the tumorigenesis of pancreatic cancer offers a new insight into the activity of metformin in hindering tumorigenicity under DM2 conditions.

Authors' contributions

G.V.T., E.F.M., H.H.C., S.C.Y., and X.M. performed the experiments. G.V.T., E.F.M., H.H.C., S.C.Y., X.M., and M.H.L. conceived and designed the study, and analysed and interpreted data. H.H.C. and M.H.L. wrote the paper with feedback from all authors. All authors reviewed and approved the final manuscript.

Funding

This research was supported in part by the National Key R&D Program of China [2018YFC0910303] Foundation, Fidelity Foundation, the National Natural Science Foundation of China [81630072], and National Key Clinical Discipline.

Conflicts of interest

None declared.

References

1. Rahib L, Smith BD, Aizenberg R et al. Projecting cancer incidence and deaths to 2030: the unexpected burden of thyroid, liver, and pancreas cancers in the United States. *Cancer Res* 2014;74:2913–21.
2. Pushalkar S, Hundeyin M, Daley D et al. The pancreatic cancer microbiome promotes oncogenesis by induction of innate and adaptive immune suppression. *Cancer Discov* 2018;8:403–16.
3. Zou S, Fang L, Lee MH. Dysbiosis of gut microbiota in promoting the development of colorectal cancer. *Gastroenterol Rep (Oxf)* 2018;6:1–12.
4. Aykut B, Pushalkar S, Chen R et al. The fungal mycobiome promotes pancreatic oncogenesis via activation of MBL. *Nature* 2019;574:264–7.

5. Abbruzzese JL, Andersen DK, Borrebaeck CAK et al. The interface of pancreatic cancer with diabetes, obesity, and inflammation: research gaps and opportunities: summary of a National Institute of Diabetes and Digestive and Kidney Diseases Workshop. *Pancreas* 2018;**47**:516–25.
6. Tilg H, Moschen AR. Microbiota and diabetes: an evolving relationship. *Gut* 2014;**63**:1513–21.
7. Andersen DK, Korc M, Petersen GM et al. Diabetes, pancreatic cancer, and pancreatic cancer. *Diabetes* 2017;**66**:1103–10.
8. Wang F, Herrington M, Larsson J et al. The relationship between diabetes and pancreatic cancer. *Mol Cancer* 2003;**2**:4.
9. Zhang AMY, Magrill J, de Winter TJJ et al. Endogenous hyperinsulinemia contributes to pancreatic cancer development. *Cell Metab* 2019;**30**:403–4.
10. Pezzilli R, Pagano N. Is diabetes mellitus a risk factor for pancreatic cancer? *World J Gastroenterol* 2013;**19**:4861–6.
11. Koenig RJ, Cerami A. Synthesis of hemoglobin A1c in normal and diabetic mice: potential model of basement membrane thickening. *Proc Natl Acad Sci USA* 1975;**72**:3687–91.
12. Ota S, Horigome K, Ishii T et al. Metformin suppresses glucose-6-phosphatase expression by a complex I inhibition and AMPK activation-independent mechanism. *Biochem Biophys Res Commun* 2009;**388**:311–6.
13. Pollak M. Metformin and pancreatic cancer: a clue requiring investigation. *Clin Cancer Res* 2012;**18**:2723–5.
14. Fuentes-Mattei E, Velazquez-Torres G, Phan L et al. Effects of obesity on transcriptomic changes and cancer hallmarks in estrogen receptor-positive breast cancer. *J Natl Cancer Inst* 2014;**106**:dju158.
15. Feng YH, Velazquez-Torres G, Gully C et al. The impact of type 2 diabetes and antidiabetic drugs on cancer cell growth. *J Cell Mol Med* 2011;**15**:825–36.
16. Corbett TH, Roberts BJ, Leopold WR et al. Induction and chemotherapeutic response of two transplantable ductal adenocarcinomas of the pancreas in C57BL/6 mice. *Cancer Res* 1984;**44**:717–26.
17. Phan L, Chou PC, Velazquez-Torres G et al. The cell cycle regulator 14-3-3sigma opposes and reverses cancer metabolic reprogramming. *Nat Commun* 2015;**6**:7530.
18. Fang L, Lu W, Choi HH et al. ERK2-dependent phosphorylation of CSN6 is critical in colorectal cancer development. *Cancer Cell* 2015;**28**:183–97.
19. Gully CP, Velazquez-Torres G, Shin JH et al. Aurora B kinase phosphorylates and instigates degradation of p53. *Proc Natl Acad Sci USA* 2012;**109**:E1513–22.
20. Qin XF, An DS, Chen IS et al. Inhibiting HIV-1 infection in human T cells by lentiviral-mediated delivery of small interfering RNA against CCR5. *Proc Natl Acad Sci USA* 2003;**100**:183–8.
21. Zou Y, Peng H, Zhou B et al. Systemic tumor suppression by the proapoptotic gene bik. *Cancer Res* 2002;**62**:8–12.
22. Zhao R, Fuentes-Mattei E, Velazquez-Torres G et al. Exenatide improves glucocorticoid-induced glucose intolerance in mice. *Diabetes Metab Syndr Obes* 2011;**4**:61–5.
23. Subramanian A, Tamayo P, Mootha VK et al. Gene set enrichment analysis: a knowledge-based approach for interpreting genome-wide expression profiles. *Proc Natl Acad Sci U S A* 2005;**102**:15545–50.
24. Chen J, Shin JH, Zhao R et al. CSN6 drives carcinogenesis by positively regulating Myc stability. *Nat Commun* 2014;**5**:5384.
25. Verdin E. NAD(+) in aging, metabolism, and neurodegeneration. *Science* 2015;**350**:1208–13.
26. Chen W, Guo JX, Chang P. The effect of taurine on cholesterol metabolism. *Mol Nutr Food Res* 2012;**56**:681–90.
27. Ames BN. Prolonging healthy aging: longevity vitamins and proteins. *Proc Natl Acad Sci USA* 2018;**115**:10836–44.
28. Warburg O, Wind F, Negelein E. The metabolism of tumors in the body. *J Gen Physiol* 1927;**8**:519–30.
29. Warburg O. On the origin of cancer cells. *Science* 1956;**123**:309–14.
30. Figueroa CD, Taberner PV. Pancreatic islet hypertrophy in spontaneous maturity onset obese-diabetic CBA/Ca mice. *Int J Biochem* 1994;**26**:1299–303.
31. Watkins SM, Reifsnnyder PR, Pan HJ et al. Lipid metabolome-wide effects of the PPARgamma agonist rosiglitazone. *J Lipid Res* 2002;**43**:1809–17.
32. Nunez NP, Oh WJ, Rozenberg J et al. Accelerated tumor formation in a fatless mouse with type 2 diabetes and inflammation. *Cancer Res* 2006;**66**:5469–76.
33. Wu PY, Yu IS, Lin YC et al. Activation of Aryl hydrocarbon receptor by kynurenine impairs progression and metastasis of neuroblastoma. *Cancer Res* 2019;**79**:5550–62.
34. Moyer BJ, Rojas IY, Kerley-Hamilton JS et al. Inhibition of the aryl hydrocarbon receptor prevents Western diet-induced obesity: model for AHR activation by kynurenine via oxidized-LDL, TLR2/4, TGFbeta, and IDO1. *Toxicol Appl Pharmacol* 2016;**300**:13–24.
35. Contador-Troca M, Alvarez-Barrientos A, Merino JM et al. Dioxin receptor regulates aldehyde dehydrogenase to block melanoma tumorigenesis and metastasis. *Mol Cancer* 2015;**14**:148.
36. Schlezinger JJ, Liu D, Farago M et al. A role for the aryl hydrocarbon receptor in mammary gland tumorigenesis. *Biol Chem* 2006;**387**:1175–87.
37. Okabe K, Yaku K, Tobe K et al. Implications of altered NAD metabolism in metabolic disorders. *J Biomed Sci* 2019;**26**:34.
38. Imai S, Guarente L. NAD+ and sirtuins in aging and disease. *Trends Cell Biol* 2014;**24**:464–71.
39. Al-Mohaisen MA, Pun SC, Frohlich JJ. Niacin: from mechanisms of action to therapeutic uses. *Mini Rev Med Chem* 2010;**10**:204–17.
40. Bogan KL, Brenner C. Nicotinic acid, nicotinamide, and nicotinamide riboside: a molecular evaluation of NAD+ precursor vitamins in human nutrition. *Annu Rev Nutr* 2008;**28**:115–30.
41. Islam J, Sato S, Watanabe K et al. Dietary tryptophan alleviates dextran sodium sulfate-induced colitis through aryl hydrocarbon receptor in mice. *J Nutr Biochem* 2017;**42**:43–50.
42. Sak D, Erdenen F, Muderrisoglu C et al. The relationship between plasma taurine levels and diabetic complications in patients with type 2 diabetes mellitus. *Biomolecules* 2019;**9**:96.
43. Sirdah MM. Protective and therapeutic effectiveness of taurine in diabetes mellitus: a rationale for antioxidant supplementation. *Diabetes Metab Syndr* 2015;**9**:55–64.
44. Ito T, Schaffer SW, Azuma J. The potential usefulness of taurine on diabetes mellitus and its complications. *Amino Acids* 2012;**42**:1529–39.
45. Kim C, Cha YN. Taurine chloramine produced from taurine under inflammation provides anti-inflammatory and cytoprotective effects. *Amino Acids* 2014;**46**:89–100.
46. Ren R, Yu J, Zhang Y et al. Inflammation promotes progression of pancreatic cancer through WNT/beta-catenin pathway-dependent manner. *Pancreas* 2019;**48**:1003–14.
47. Gomez-Chou SB, Swidnicka-Siergiejko AK, Badi N et al. Lipocalin-2 promotes pancreatic ductal adenocarcinoma by regulating inflammation in the tumor microenvironment. *Cancer Res* 2017;**77**:2647–60.
48. Asano K, Suzuki T, Saito A et al. Metabolic and chemical regulation of tRNA modification associated with taurine deficiency and human disease. *Nucleic Acids Res* 2018;**46**:1565–83.

49. Tang Y, Kim YS, Choi EJ et al. Taurine attenuates epithelial-mesenchymal transition-related genes in human prostate cancer cells. *Adv Exp Med Biol* 2017;**975 Pt 2**:1203–12.
50. Sarkar P, Basak P, Ghosh S et al. Prophylactic role of taurine and its derivatives against diabetes mellitus and its related complications. *Food Chem Toxicol* 2017;**110**:109–21.
51. Glunde K, Bhujwala ZM, Ronen SM. Choline metabolism in malignant transformation. *Nat Rev Cancer* 2011;**11**:835–48.
52. Chen X, Qiu H, Wang C et al. Molecular structure and differential function of choline kinases CHKalpha and CHKbeta in musculoskeletal system and cancer. *Cytokine Growth Factor Rev* 2017;**33**:65–72.